Nanoductility in silicate glasses is driven by topological heterogeneity

Bu Wang,[1] Yingtian Yu,[1] Mengyi Wang,[1] John C. Mauro,[2] and Mathieu Bauchy[1,*]

[1]*Physics of AmoRphous and Inorganic Solids Laboratory (PARISlab), Department of Civil and Environmental Engineering, University of California, Los Angeles, California, USA*

[2]*Science and Technology Division, Corning Incorporated, Corning, New York 14831, USA*

(Received 8 July 2015; revised manuscript received 26 January 2016; published 9 February 2016)

The existence of nanoscale ductility during the fracture of silicate glasses remains controversial. Here, based on molecular dynamics simulations coupled with topological constraint theory, we show that nanoductility arises from the spatial heterogeneity of the atomic network's rigidity. Specifically, we report that localized floppy modes of deformation in underconstrained regions of the glass enable plastic deformations of the network, resulting in permanent change in bond configurations. Ultimately, these heterogeneous plastic events percolate, thereby resulting in a nonbrittle mode of fracture. This suggests that nanoductility is intrinsic to multicomponent silicate glasses having nanoscale heterogeneities.

DOI: 10.1103/PhysRevB.93.064202

I. INTRODUCTION

Although silicate glasses are commonly viewed as archetypal brittle materials, the existence of metal-like ductility at the nanoscale has recently been suggested [1–4]. This has both fundamental and practical importance, as increasing such ductility would allow one to design tougher glasses. Such glasses, more resistant to fracture while retaining their transparency, would broadly expand the range of applications for glasses [5].

However, the existence of nanoductility in glass remains highly debated. Celarie first reported the observation of nanoductility in an aluminosilicate glass via fractured surface topographical analysis [1]. However, a later study using atomic force microscopy mapping the fractured surfaces of silica and soda-lime glass did not find any evidence of such a ductile failure [6] and neither did cathodoluminescence spectroscopy measurements on silica [7]. In an effort to resolve this debate, simulations have also been conducted to explore the relationship between ductility and fine structural details, e.g., nanocavities [2,8,9], or material properties, e.g., the Poisson's ratio [3]. In particular, our recent study showed that the composition of glass plays a critical role in determining the existence of nanoductility [4]. We reported that pure silica breaks in a nearly perfectly brittle manner, while the fracture of multicomponent glasses such as sodium silicate and calcium aluminosilicate exhibit significant ductility [4]. Such a compositional dependence, which might have partly contributed to the discrepancies among experiments, is in agreement with experimental results obtained for sodium silicate glasses [10].

Aside from the extrinsic origins theorized in previous studies, e.g., stress corrosion cracking with the presence of water [6,11–13] or macroscopic defects [2], questions remain regarding the atomistic origin of such nanoductility for suitable compositions of glass. In particular, spectroscopy analyses revealed the existence of an excess of alkali network modifier atoms in as-fractured surfaces of silicate glass [14], which suggests that crack propagation may preferentially occur along alkali-rich regions, in agreement with the picture offered by Greaves' modified random network [15]. Such spatial fluctuation of alkali's concentration could induce heterogeneities in the network's local rigidity [16], which, in turn, can result in crack deflection [17] and ductility. To this end, we conduct molecular dynamics simulations coupled with topological constraint theory [18–20] on $(Na_2O)_{20}(SiO_2)_{80}$ glasses (hereafter denoted as 20NS) to elucidate the effect of network rigidity at nanoscale on the fracture behavior of multicomponent glasses.

Topological constraint theory has proven to be a powerful tool to evaluate the important rigidity of atomic networks, while filtering out the chemical details that ultimately do not affect macroscopic properties [18–20]. As such, it has provided critical understanding of the atomic origins of various phenomena in glasses, such as fracture statistics and composition-dependent hardness [21–25]. Analogous to mechanical trusses, the rigidity of an atomic network can be evaluated by enumerating the number of constraints per atom (n_c), which includes bond-stretching and bond-bending constraints, and comparing this metrics with the number of degrees of freedom per atom (three for three-dimensional networks). Underconstrained structures ($n_c < 3$, flexible) contain extra internal degrees of freedom ($f = 3 - n_c$, floppy modes [26]) and thereby feature low-energy modes of deformation [27], which allow flexibility in atomic rearrangement and structural relaxation. In contrast, overconstrained structures ($n_c > 3$, stressed rigid) become rigid and undergo internal eigenstress [28]. In between, the existence of an isostatic intermediate phase has also been suggested [29], in which networks are rigid but free of eigenstress [30] or consist of a combination of rigid and floppy regions [31]. Such isostatic glasses have been shown to feature maximal fracture toughness [32], which suggests that the resistance to fracture is related to the atomic topology [25].

As will be discussed later, sodium silicate glass goes through a rigidity transition at sodium oxide concentration of 20% [33–35], therefore the 20NS chosen here exhibit isostatic behavior at the microscopic scale. However, based on simulation results, we show that the spatial fluctuations of alkali's concentration naturally existing in multicomponent

*Corresponding author: bauchy@ucla.edu; http://mathieu.bauchy.com

glasses induce heterogeneities in the network's local rigidity [16], creating under- and overconstrained regions at nanoscale. This, in turn, can result in excessive plastic deformations in the flexible, underconstrained regions and ductility. Overall, our results suggest that nanoductility is intrinsic to multicomponent silicate glasses and originates from topological heterogeneities.

II. METHODS

The simulations are carried out using the LAMMPS package [36]. Several classical potential sets are available for the simulation of sodium silicate glasses [37–41]. We adopt a Buckingham potential set parametrized by Teter [38]. The potential has been shown to provide realistic results for structure, dynamics, and mechanics of sodium silicate glasses [16,42–45].

Glass structures of 20NS containing 9000 atoms are first obtained by melting random atomic configurations at 4000 K for 1 ns and then quenching the glass-forming liquids to 300 K with 1 K/ps cooling rate, all in NPT ensemble with zero pressure. After an equilibration at 300 K for 1 ns under zero pressure, the simulation box is gradually stretched by stepwise 0.5% (∼0.25 Å) increases along the z direction, until the structure is fully fractured. During each step, the structure is first stretched by linearly scaling the atomic coordinates. The system is then relaxed for 50 ps before a statistical averaging phase of 50 ps, all in the NVT ensemble. Note that, rather than mimicking standard notched tests for measuring fracture toughness, we aim to observe the spontaneous global response of the system to a tensile stress. As such, no notch is inserted here, as it would arbitrarily concentrate the stress in a predetermined region of the glass. For statistics, six individual simulations are performed.

III. RESULTS

Figure 1 shows an example of the computed tensile stress with respect to the applied strain during the fracture. In agreement with what was observed for 30NS [4], 20NS exhibits a nonbrittle fracture behavior, i.e., the stress does not suddenly decrease to zero after reaching its maximum, when the crack starts to propagate. Such behavior strongly contrasts with that observed for the fracture of pure silica, in which a sudden drop of stress is observed (see Fig. 1). The simulation reveals the existence of cavities that form during the fracture, as typically observed for ductile materials. Indeed, as shown in Fig. 1 for a series of strains, the fracture clearly happens through cavity initiation, growth, and eventually, coalescence. This mechanism is in agreement with previous simulations, which report that nanoductility arises from preexisting, nanosized voids in aluminosilicate [2] and pure silica [10,46,47]. Here, in the case of sodium silicate, we show that the formation of such cavities can naturally happen, even without preexisting microscopic flaws, such as cavities and microcracks. Similar observations have also been made in molecular dynamics simulations of sodium borosilicate glasses [48]. We note, however, that one should be cautious about using such phenomenological observation in experiment to qualify the nature of the fracture, especially

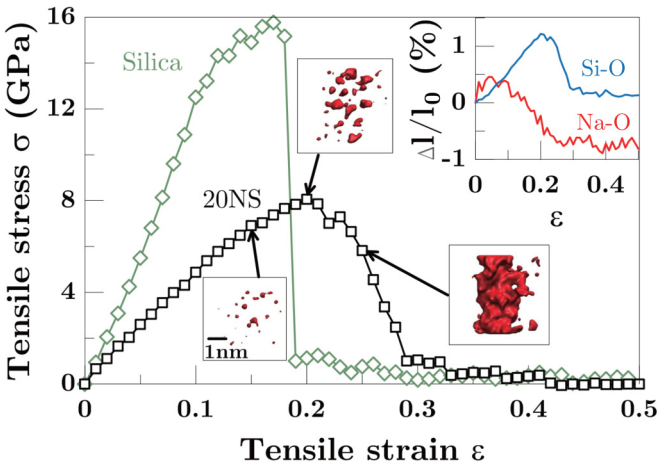

FIG. 1. Example stress-strain response of the simulated $(Na_2O)_{20}(SiO_2)_{80}$ glass during fracture, compared with that of pure silica. The snapshots illustrate the volume of the cavities, with a radius larger than 5 Å, that are formed at various strains. The inset shows the relative variation of the average Si-O and Na-O bond lengths ($\Delta l/l_0$) with respect to the strain. The cutoffs used to identify Si-O and Na-O bonds are 1.974 and 3.311 Å, respectively, as determined from the position of the first minimum after the peak associated to the first coordination shell in the pair distribution functions.

from surface measurements. Indeed, as cavities formation and crack propagation occur in the bulk volume, it would be challenging to distinguish newly formed voids, appearing in front of the crack tip, from cracks propagating perpendicular to the surface. Interestingly, advanced post mortem analysis has revealed that brittle polymeric glass can fracture through microcrack nucleation and coalescence, which is similar to the fracture mechanism observed here for silicate glass [49].

Such a fracture, occurring via cavity initiation and coalescence, is direct evidence that the glass should not be treated as a homogeneous material at the nanoscale. Indeed, at this scale, the composition in sodium silicate is inherently nonhomogeneous [50]. The disordered structure of silicate glasses consists of a network of SiO_4 tetrahedra forming some rings [51]. Network modifier cations, such as sodium, depolymerize the Si-O network and thereby increase the average ring size [42,52]. Studies focusing on the medium range structure of silicate glasses have identified as large as 20-member rings in 20NS [42], which give rise to spatial fluctuations of composition [16,42]. On the other hand, it has been established that, for $(Na_2O)_x(SiO_2)_{1-x}$ glasses, the rigidity of the structure, as indicated by the number of constraints per atom (n_c), directly depends on the composition [18,33–35]:

$$n_c = (11 - 10x)/3. \quad (1)$$

As a result, the inhomogeneity in the local fraction of sodium oxide x induces some variations in the local structural rigidity. Such heterogeneity is demonstrated by the n_c contour map in Fig. 2. We can see that, for 20NS, substantial spatial variations of the structural rigidity exist within the glass, when the spatial resolution is kept below 15 Å.

As described by Eq. (1), sodium silicate glass goes through a rigidity transition at sodium oxide concentration of 20%

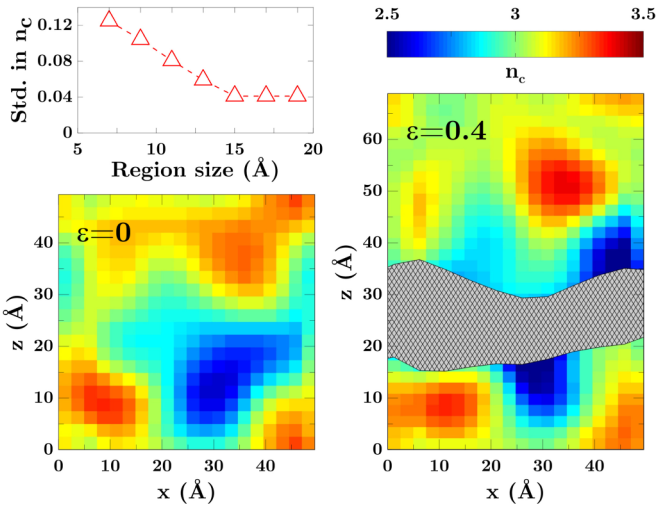

FIG. 2. Contour maps of the local number of constraints per atom (n_c) over a 8-Å-thick slab inside an example 20NS structure, before (left, $\epsilon = 0$) and after (right, $\epsilon = 0.4$) fracture. Other simulated samples show similar behavior. n_c is calculated from the local sodium oxide concentration on a square grid of 8 Å in resolution. The gray area indicates the extent of the final crack. The plot on the upper left corner shows the standard deviation of n_c as a function of the grid resolution.

[33–35]. At lower sodium oxide concentration, the structure is stressed rigid and has limited ability to rearrange and relax. On the contrary, above 20% sodium oxide, in the flexible regime, some floppy modes of deformation are available for the atomic structure to rearrange. Additionally, the existence of an isostatic intermediate phase has been reported for sodium oxide concentrations between 18% and 23% [35,53], corresponding to a theoretical n_c between 3.07 and 2.90. As such, we find that, although the 20NS composition should be isostatic, on average, at the macroscale, the compositional variations at the nanoscale result in the formation of flexible and stress-rigid regions in the glass, as illustrated in Fig. 2. Since the flexible regions feature a lower structural rigidity, they should undergo noticeable relaxation under strong stress, as experienced during the fracture.

A comparison of the atomic structures before and after fracture supports such conclusion. Indeed, during the fracture, cavities preferentially form in the flexible regions and, eventually, lead to a preferred crack propagation through these regions (see Fig. 2). This is in agreement with experimental observations [14]. In addition, the fluctuations of the local composition also result in heterogeneity of bonding, as Na-O bonds are much more ionic and weaker than the Si-O ones. As such, these two kinds of bonds behave drastically differently under strain. As shown in the inset of Fig. 1, as the strain increases, the relative deformation of Si-O bonds presents the same shape as that of the stress-strain curve, and eventually goes back to its initial zero-stress value. This means that Si-O bonds essentially deform in a reversible elastic fashion under stress. On the other hand, the Na-O bonds behave in a significantly different way. Indeed, the maximum relative elongation of the Na-O bonds is much lower than that of the Si-O bonds, which shows that, after a short elastic regime, these bonds yield at low stress and, thereby, initiate the fracture through some plastic deformations prior to the failure of any Si-O bond. This suggests that the observed nanoductility mainly arises from Na-O bonds and, therefore, should be very limited or nonexistent in pure silica.

In addition to their bond lengths, the connectivity of Si and Na atoms is also affected differently during the fracture. Indeed, most of the Si atoms (>99.9%) remain fourfold coordinated after the fracture. Most of them also retain the same O neighbors throughout the fracture process, as only a small fraction (1.5%) acquire new neighbors, mostly as a result of local relaxations at the fresh surface formed after fracture. On the contrary, around 90% of the Na atoms switch their oxygen neighbor during the fracture, even though the average coordination number only shows a moderate change (from 5.94 to 5.46). Such exchanges of neighbors are irreversible, which clearly shows that a significant number of plastic deformations happen around Na atoms. It is also worth noting that the local relaxation around Na atoms can happen at stresses much lower than the strength of the glass. This feature echoes with the flexible nature of Na-O polyhedra [33], and may be related to the observed relaxation of alkali silicate glasses at low temperature [54,55]. Finally, bond angles are also affected during the fracture. Previous studies have shown that the Si-O network can undergo deformations during fracture [12,56,57]. We find that, although strong intratetrahedral O-Si-O angles remain largely unaffected, a fraction of the weaker intertetrahedral Si-O-Si angles experience a permanent change of their average value after fracture, which suggests that some plastic deformations occur in the Si-O network.

Based on these observations, we classify and quantify the fracture-induced plastic events happening in the environment of (1) the bridging oxygen (BO) species, i.e., O linked to two Si

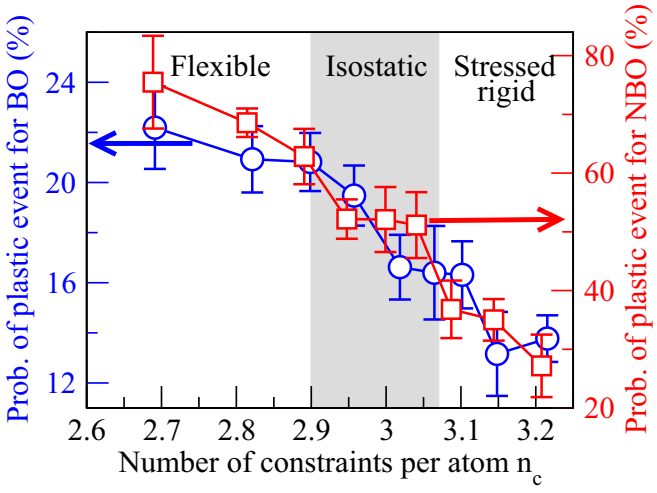

FIG. 3. Probabilities of plastic events (see text) occurring around the bridging (BO, open circles) and nonbridging (NBO, open squares) oxygen atoms with respect to the local number of constraints per atom n_c. The sampling frequency in terms of n_c is chosen so that each group contains at least 500 oxygen atoms. The error bars are obtained from six individual simulations. The gray area indicates the boundaries of the intermediate phase observed experimentally through modulated differential scanning calorimetry [35,53].

atoms, and (2) the nonbridging oxygen (NBO) species, i.e., O linked to one Si atom and at least one Na atom. (1) The number of plastic events affecting BOs is defined as the number of Si-BO-Si angles that show a significant permanent distortion of at least 15%. (2) The number of plastic events affecting NBOs is defined as the number of oxygen atoms that lose at least half of their initial Na neighbors. The probabilities of these plastic events are then correlated to the local rigidity experienced around the oxygen species, as obtained by calculating n_c within an 8-Å-radius sphere centered around the considered O, using Eq. (1).

As shown in Fig. 3, both for BOs and NBOs, the probability of plastic events decreases with increasing local rigidity, as captured by n_c, which shows that ductility is mainly concentrated in the flexible regions. Interestingly, the probability of such events shows a plateau in the stressed-rigid domain. Such a trend appears similar to the fraction of floppy modes observed in chalcogenide glasses [58–60], which suggests that plastic events arise from such low-energy modes of deformation.

IV. SUMMARY

Overall, the results presented here are consistent with the following topological picture. Thanks to internal degrees of freedom, the flexible regions feature plastic deformations. On the contrary, due to the high number of constraints, stressed-rigid regions are locked and unable to reorganize under stress. Eventually, due to the heterogeneity of the local rigidity, plastic events occur in different regions of the glass, and ultimately merge to form the crack, resulting in a nanoductile fracture. On the contrary, pure silica glass shows very limited heterogeneity, and thereby breaks in a brittle way through a catastrophic failure of Si-O bonds. This also suggests that heterogeneous multicomponent glasses that are isostatic overall should feature the highest amount of nanoductility. Indeed, flexible glasses feature a large amount of flexible domains, percolating through the bulk structure, which should decrease the probability of crack deflections. On the contrary, stressed-rigid glasses possess a low amount of flexible domains, which limits the number of possible plastic events.

Since the heterogeneity of topological constraints remains limited to a nanometric scale, this nanoductility is unlikely to result in micro- or macroductility [61]. Nevertheless, more complex glasses characterized by phase separation or long-range heterogeneity could be considered to maximize this ductility, and thereby increase the resistance to fracture [50]. Pressure, as applied during quenching, can also affect heterogeneity and, consequently, nanoductility. Indeed, pressure has been found to lower the extent of topological heterogeneity in sodium silicate [16], which results in a more brittle fracture [25]. Pressure is, on the contrary, thought to induce microheterogeneity in pure silica [62] and, therefore, appears to be a promising degree of freedom to tune the ductility of glasses [63].

ACKNOWLEDGMENTS

The authors acknowledge financial support for this research provisioned by the University of California, Los Angeles (UCLA). Access to computational resources was provisioned by the Physics of AmoRphous and Inorganic Solids Laboratory (PARISlab).

[1] F. Celarie, S. Prades, D. Bonamy, L. Ferrero, E. Bouchaud, C. Guillot, and C. Marliere, Phys. Rev. Lett. **90**, 075504 (2003).
[2] Y.-C. Chen, Z. Lu, K.-i. Nomura, W. Wang, R. K. Kalia, A. Nakano, and P. Vashishta, Phys. Rev. Lett. **99**, 155506 (2007).
[3] Y. Shi, J. Luo, F. Yuan, and L. Huang, J. Appl. Phys. **115**, 043528 (2014).
[4] B. Wang, Y. Yu, Y. J. Lee, and M. Bauchy, Frontiers Mater. **2**, 11 (2015).
[5] J. C. Mauro, Frontiers Mater. **1**, 20 (2014).
[6] J.-P. Guin and S. M. Wiederhorn, Phys. Rev. Lett. **92**, 215502 (2004).
[7] G. Pezzotti and A. Leto, Phys. Rev. Lett. **103**, 175501 (2009).
[8] L. V. Brutzel, C. L. Rountree, R. K. Kalia, A. Nakano, and P. Vashishta, in *MRS Proceedings* (Cambridge University Press, Cambridge, 2001), Vol. 703, pp. V3–V9.
[9] C. Rountree, S. Prades, D. Bonamy, E. Bouchaud, R. Kalia, and C. Guillot, Proceedings of the 12th International Symposium on Metastable and Nanomaterials (ISMANAM-2005) [J. Alloys Compd. **434–435**, 60 (2007)].
[10] D. Bonamy, S. Prades, L. Ponson, D. Dalmas, C. L. Rountree, E. Bouchaud, and C. Guillot, Int. J. Mater. Prod. Technol. **26**, 339 (2006).
[11] F. Lechenault, C. L. Rountree, F. Cousin, J. P. Bouchaud, L. Ponson, and E. Bouchaud, J. Phys.: Conf. Ser. **319**, 012005 (2011).
[12] F. Lechenault, C. L. Rountree, F. Cousin, J.-P. Bouchaud, L. Ponson, and E. Bouchaud, Phys. Rev. Lett. **106**, 165504 (2011).
[13] M. M. Smedskjaer and M. Bauchy, Appl. Phys. Lett. **107**, 141901 (2015).
[14] R. M. Almeida, R. Hickey, H. Jain, and C. G. Pantano, J. Non-Cryst. Solids **385**, 124 (2014).
[15] G. N. Greaves, J. Non-Cryst. Solids **71**, 203 (1985).
[16] M. Bauchy and M. Micoulaut, Europhys. Lett. **104**, 56002 (2013).
[17] B. R. Lawn, N. P. Padture, H. Cait, and F. Guiberteau, Science **263**, 1114 (1994).
[18] J. C. Mauro, Am. Ceram. Soc. Bull. **90**, 31 (2011).
[19] J. C. Phillips, J. Non-Cryst. Solids **34**, 153 (1979).
[20] J. C. Phillips, J. Non-Cryst. Solids **43**, 37 (1981).
[21] M. Bauchy, Mohammad Javad Abdolhosseini Qomi, C. Bichara, F.-J. Ulm, and Roland J.-M. Pellenq, Phys. Rev. Lett. **114**, 125502 (2015).
[22] J. C. Mauro and M. M. Smedskjaer, Phys. A (Amsterda, Neth.) **391**, 6121 (2012).
[23] M. M. Smedskjaer, Front. Mater. **1**, 23 (2014).
[24] M. M. Smedskjaer, J. C. Mauro, and Y. Yue, Phys. Rev. Lett. **105**, 115503 (2010).
[25] M. Bauchy, M. J. Abdolhosseini Qomi, C. Bichara, F.-J. Ulm, and R.-M. Pellenq, arXiv:1410.2916.
[26] G. G. Naumis, Phys. Rev. E **71**, 026114 (2005).

[27] Y. Cai and M. F. Thorpe, Phys. Rev. B **40**, 10535 (1989).
[28] F. Wang, S. Mamedov, P. Boolchand, B. Goodman, and M. Chandrasekhar, Phys. Rev. B **71**, 174201 (2005).
[29] P. Boolchand, D. Georgiev, and B. Goodman, J. Opt. Adv. Mater. **3**, 703 (2001).
[30] M. Micoulaut and J. C. Phillips, J. Non-Cryst. Solids **353**, 1732 (2007).
[31] M. V. Chubynsky, M. A. Briere, and N. Mousseau, Phys. Rev. E **74**, 016116 (2006).
[32] A. K. Varshneya and D. J. Mauro, J. Non-Cryst. Solids **353**, 1291 (2007).
[33] M. Bauchy and M. Micoulaut, J. Non-Cryst. Solids **357**, 2530 (2011).
[34] M. F. Thorpe, J. Non-Cryst. Solids **57**, 355 (1983).
[35] Y. Vaills, T. Qu, M. Micoulaut, F. Chaimbault, and P. Boolchand, J. Phys.: Condens. Matter **17**, 4889 (2005).
[36] S. Plimpton, J. Comput. Phys. **117**, 1 (1995).
[37] J. Horbach, W. Kob, and K. Binder, 6th International Silicate Melt Workshop [Chem. Geol. **174**, 87 (2001)].
[38] A. N. Cormack, J. Du, and T. R. Zeitler, Phys. Chem. Chem. Phys. **4**, 3193 (2002).
[39] A. Tilocca, N. H. de Leeuw, and A. N. Cormack, Phys. Rev. B **73**, 104209 (2006).
[40] A. Pedone, G. Malavasi, M. C. Menziani, A. N. Cormack, and U. Segre, J. Phys. Chem. B **110**, 11780 (2006).
[41] B. Guillot and N. Sator, Geochim. Cosmochim. Acta **71**, 1249 (2007).
[42] J. Du and A. Cormack, J. Non-Cryst. Solids **349**, 66 (2004).
[43] A. Pedone, G. Malavasi, A. N. Cormack, U. Segre, and M. C. Menziani, Chem. Mater. **19**, 3144 (2007).
[44] M. Bauchy and M. Micoulaut, Phys. Rev. B **83**, 184118 (2011).
[45] M. Bauchy, J. Chem. Phys. **137**, 044510 (2012).
[46] Z. Lu, K.-i. Nomura, A. Sharma, W. Wang, C. Zhang, A. Nakano, R. Kalia, P. Vashishta, E. Bouchaud, and C. Rountree, Phys. Rev. Lett. **95**, 135501 (2005).
[47] S. Prades, D. Bonamy, D. Dalmas, E. Bouchaud, and C. Guillot, Int. J. Solids Struct. **42**, 637 (2005).
[48] L.-H. Kieu, J.-M. Delaye, and C. Stolz, J. Non-Cryst. Solids **358**, 3268 (2012).
[49] C. Guerra, J. Scheibert, D. Bonamy, and D. Dalmas, Proc. Natl. Acad. Sci. USA **109**, 390 (2012).
[50] J. C. Mauro, J. Chem. Phys. **138**, 12A522 (2013).
[51] C. S. Marians and L. W. Hobbs, J. Non-Cryst. Solids **124**, 242 (1990).
[52] J. Du and L. R. Corrales, Phys. Rev. B **72**, 092201 (2005).
[53] M. Micoulaut, Am. Mineral. **93**, 1732 (2008).
[54] R. C. Welch, J. R. Smith, M. Potuzak, X. Guo, B. F. Bowden, T. J. Kiczenski, D. C. Allan, E. A. King, A. J. Ellison, and J. C. Mauro, Phys. Rev. Lett. **110**, 265901 (2013).
[55] Y. Yu, M. Wang, D. Zhang, B. Wang, G. Sant, and M. Bauchy, Phys. Rev. Lett. **115**, 165901 (2015).
[56] L.-H. Kieu, Ph.D. thesis, Ecole Polytechnique, France, 2011.
[57] C. L. Rountree, D. Vandembroucq, M. Talamali, E. Bouchaud, and S. Roux, Phys. Rev. Lett. **102**, 195501 (2009).
[58] W. A. Kamitakahara, R. L. Cappelletti, P. Boolchand, B. Halfpap, F. Gompf, D. A. Neumann, and H. Mutka, Phys. Rev. B **44**, 94 (1991).
[59] J. C. Mauro and A. K. Varshneya, J. Am. Ceram. Soc. **90**, 192 (2007).
[60] J. C. Mauro and A. K. Varshneya, J. Non-Cryst. Solids **353**, 1226 (2007).
[61] S. Vernède, L. Ponson, and J.-P. Bouchaud, Phys. Rev. Lett. **114**, 215501 (2015).
[62] J. Arndt and D. Stöffler, Phys. Chem. Glasses **10**, 117 (1969).
[63] F. Yuan and L. Huang, Sci. Rep. **4**, 5035 (2014).